

22. D. W. Banner *et al.*, *Cell* **73**, 431 (1993).

23. An enriched T lymphocyte population was isolated from peripheral blood by Ficoll-Hypaque centrifugation, incubation on plastic to deplete adherent cells, and depletion of B lymphocytes with anti-CD19-conjugated magnetic beads (Dyna) before culture.

24. Y. Takebe *et al.*, *Mol. Cell. Biol.* **8**, 466 (1988).

25. Interaction was demonstrated by growth of yeast on histidine-deficient medium in the presence of 50 mM 3-amino triazole and was verified by activation of a gal-lacZ reporter (2).

26. Supported by NIH grant CA21765, ACS grant BE-

234, and by the American Lebanese Syrian Associated Charities. R.J.B. was a James S. McDonnell Foundation Scholar in the program for Molecular Medicine in Cancer Research.

19 May 1997; accepted 8 August 1997

Evidence for a Role of CRM1 in Signal-Mediated Nuclear Protein Export

Batool Ossareh-Nazari, Françoise Bachelerie, Catherine Dargemont*

Chromosome maintenance region 1 (CRM1), a protein that shares sequence similarities with the karyopherin β family of proteins involved in nuclear import pathway, was shown to form a complex with the leucine-rich nuclear export signal (NES). This interaction was inhibited by leptomycin B, a drug that prevents the function of the CRM1 protein in yeast. To analyze the role of the CRM1-NES interaction in nuclear export, a transport assay based on semipermeabilized cells was developed. In this system, which reconstituted NES-, cytosol-, and energy-dependent nuclear export, leptomycin B specifically blocked export of NES-containing proteins. Thus, the CRM1 protein could act as a NES receptor involved in nuclear protein export.

Bidirectional transport across the nuclear envelope occurs through nuclear pore complexes. This process requires specific sequences found within transport substrates, soluble transport proteins, and nucleoporins. Thus, the import of nuclear proteins is governed by different nuclear localization sequences (NLS) that are presumably recognized by distinct receptors (karyopherins, importins, and transportins) that mediate the docking of the transport substrate at the cytoplasmic face of the nuclear pore (1) and by other soluble factors, including the small guanosine triphosphatase Ran and p10, that are responsible for the translocation step across the nuclear pore complex (2). Recent studies have shown that soluble factors involved in the docking step of nuclear import and in Ran-binding ability share amino acid sequences and structural homology domains. The CRM1 protein shares sequence homology in its NH₂-terminal region with the karyopherin β family, as well as with the Ran-guanosine triphosphate (GTP)-binding domain of the Ran-GTP-binding protein family. This protein, which is encoded by an essential gene in yeast, is located at the nuclear pore complex as well as in the nucleoplasm (3, 4). Thus, we examine whether CRM1 could be involved in nuclear export.

Although most nuclear proteins are po-

tential shuttling proteins (5), amino acid sequences responsible for highly efficient nuclear export (NES) have recently been identified in an increasing number of proteins, in particular, the human immunodeficiency virus-type 1 (HIV-1) Rev protein, the protein kinase A inhibitor I κ B α , and the heterogeneous nuclear ribonucleopro-

teins (hnRNPs) A1 and K (6). With the exception of the hnRNPs, NES is a leucine-rich sequence in which leucine residues are critical for targeting proteins out of the nucleus. Molecular mechanisms governing NES-dependent nuclear protein export are less well documented than those of the nuclear protein import pathway. However, the existence of NES as well as its ability to saturate NES-dependent export strongly suggest the involvement of specific NES receptors in this process.

To analyze the role of CRM1 in nuclear protein export, we first tested the ability of human CRM1 protein to bind a leucine-rich sequence (NES) (7). For this purpose, interaction of human CRM1 with wild-type I κ B α or I κ B α -L234, a nuclear export mutant of I κ B α in which leucine residues of NES have been replaced by alanine (6, 8), was analyzed. *In vitro*-translated human MYC-tagged CRM1 was mixed with *in vitro*-translated SV5-tagged wild-type I κ B α or I κ B α -L234 before being processed for immunoprecipitation with an antibody to the MYC tag (anti-MYC tag) or an anti-SV5 tag. CRM1 protein and wild-type I κ B α coprecipitated with both an-

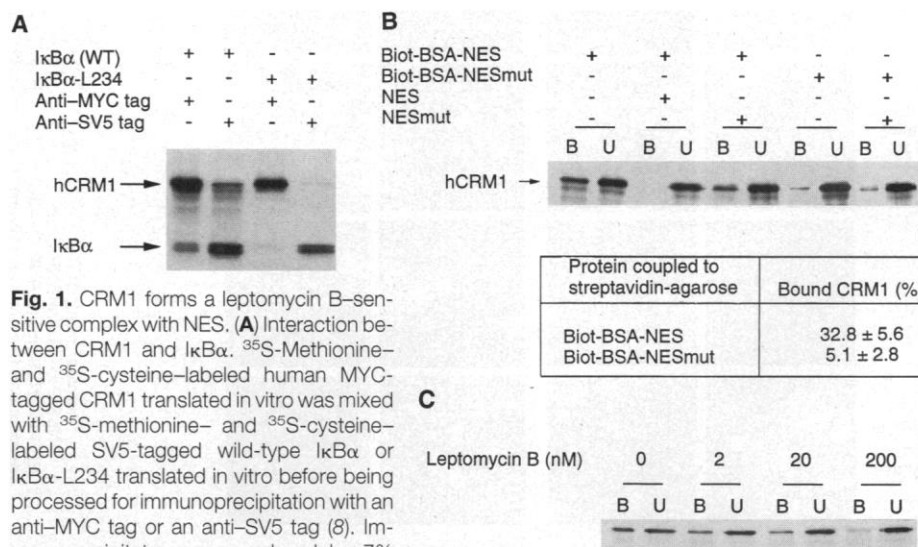


Fig. 1. CRM1 forms a leptomycin B-sensitive complex with NES. **(A)** Interaction between CRM1 and I κ B α . ³⁵S-Methionine- and ³⁵S-cysteine-labeled human MYC-tagged CRM1 translated *in vitro* was mixed with ³⁵S-methionine- and ³⁵S-cysteine-labeled SV5-tagged wild-type I κ B α or I κ B α -L234 translated *in vitro* before being processed for immunoprecipitation with an anti-MYC tag or an anti-SV5 tag (8). Immunoprecipitates were analyzed by 7% SDS-PAGE and autoradiography. **(B)** Interaction between CRM1 and NES. ³⁵S-Methionine- and ³⁵S-cysteine-labeled CRM1 translated *in vitro* was incubated with streptavidin-agarose beads bound to biotinylated BSA-NES (biot-BSA-NES) or mutated NES (biot-BSA-NESmut) conjugates (8). The binding was performed with or without NES or mutated NES (NESmut) peptides (each 2 mg/ml). Bound (B) and unbound (U) fractions were collected and analyzed by 7% SDS-PAGE and autoradiography. The Bioprint acquisition system and Bioprofil program were used to quantify the autoradiograms. Values were obtained from five independent experiments. **(C)** ³⁵S-Methionine- and ³⁵S-cysteine-labeled CRM1 translated *in vitro* was incubated with streptavidin-agarose beads bound to biotinylated BSA-NES conjugate (30 min at room temperature in PBS) with increasing concentrations of leptomycin B. Bound and unbound fractions were collected and analyzed by 7% SDS-PAGE and autoradiography.

B. Ossareh-Nazari and C. Dargemont, Institut Curie-CNRS Unité Mixte de Recherche 144, 26 rue d'Ulm, 75248 Paris Cedex 05, France.
F. Bachelerie, Institut Pasteur, Unité d'Immunologie Virale, 75015 Paris, France.

*To whom correspondence should be addressed. E-mail: dargemont@curie.fr

tibodies. In contrast, no coprecipitation was observed between CRM1 and $\text{I}\kappa\text{B}\alpha$ -L234 (Fig. 1A), which suggests that CRM1 interacts with $\text{I}\kappa\text{B}\alpha$ NES. To confirm this result, we conjugated biotinylated bovine serum albumin (BSA) to $\text{I}\kappa\text{B}\alpha$ NES (CIQQQLGQLTLENL) or mutated NES (CIQQQAGQATAENA) (9) peptides and coupled it to streptavidin-agarose. In vitro-translated human CRM1 bound to a NES affinity column. However, no binding of CRM1 was observed when leucine residues of NES were substituted by alanines (Fig. 1B) (8) or when NES was replaced by NLS (10). Under the same experimental conditions, no specific binding was observed between NES and in vitro-translated human RIP (10). CRM1-NES interaction was prevented by the addition of an excess of NES peptide but was not affected by the mutated NES (Fig. 1B), which confirms that CRM1 interacts specifically with NES. However, the possibility that the specific interaction between CRM1 and NES could be mediated by a factor provided by reticulocyte lysate cannot be formally excluded.

The CRM1 homolog in *Schizosaccharomyces pombe* is the target of leptomycin B, an antifungal antibiotic that induces cell

cycle arrest at the G_1 and G_2 phases in both mammalian and fission yeast cells (11). To test whether the leptomycin B-induced inhibition of CRM1 function was related to the ability of CRM1 to bind NES, we monitored the effect of the drug on CRM1-NES interaction. Addition of leptomycin B to 200 nM concentration completely blocked the formation of CRM1-NES complexes (Fig. 1C). We controlled the leptomycin B so that it did not bind directly to NES (10). Thus, CRM1 protein bound NES specifically in a leptomycin B-sensitive manner.

To analyze the role of the CRM1-NES interaction in the export of nuclear proteins, we developed an assay that reconstitutes nuclear export in vitro. HeLa cells were transiently transfected with cDNAs encoding fusion proteins consisting of MYC-tagged pyruvate kinase (PK), wild-type or mutated $\text{I}\kappa\text{B}\alpha$ NES, and SV40 large T antigen NLS to direct the resulting proteins to the nucleus (NLS-PK-NES and NLS-PK-NESmut, respectively) (12). Eighteen hours after transfection, cells were treated with digitonin to permeabilize the plasma membrane and remove cytosolic components without affecting the integrity

of the nuclear envelope (13). Exports of NLS-PK-NES and NLS-PK-NESmut from permeabilized cell nuclei were analyzed under different incubation conditions by indirect immunofluorescence with an anti-MYC tag (Fig. 2A) (14). Incubation of permeabilized cells with buffer in the presence or absence of adenosine triphosphate (ATP) did not allow nuclear export of both proteins. In contrast, addition of *Xenopus laevis* egg extracts (cytosol) and ATP for 30 min at 23°C led to the disappearance of NLS-PK-NES from the nucleus, whereas the nuclear content of NLS-PK-NESmut was not affected. Treatment of the cytosol with apyrase abolished the disappearance of NLS-PK-NES from the nucleus. Because only a few amino acids within NES are different between both proteins, the disappearance of NLS-PK-NES from the nucleus treated with cytosol and ATP likely corresponded to an active nuclear export of this protein rather than an ATP-dependent hydrolysis that should also affect the mutated protein. To quantify results obtained by indirect immunofluorescence, we analyzed proteins from permeabilized cells treated in the different conditions by SDS-polyacryl-

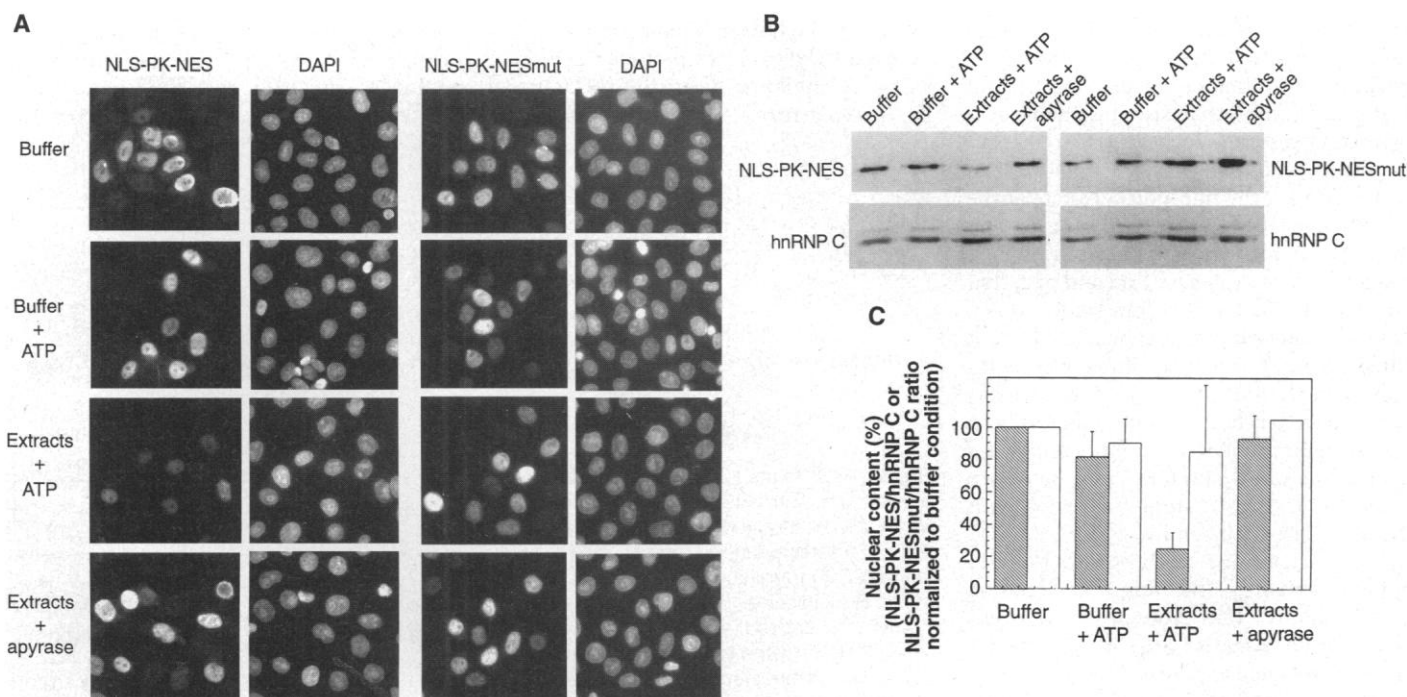


Fig. 2. In vitro NES-dependent protein nuclear export assay. HeLa cells were transiently transfected with cDNAs encoding NLS-PK-NES or NLS-PK-NESmut (12). Eighteen hours after transfection, cells were permeabilized with digitonin (55 $\mu\text{g}/\text{ml}$) in transport buffer and incubated for 30 min at 23°C with BSA (20 mg/ml) in transport buffer in the absence (buffer) or presence of ATP (buffer + ATP) or with 45% *X. laevis* egg extracts in transport buffer in the presence of ATP (extracts + ATP) or in the absence of ATP [addition of apyrase (20 U/ml); extracts + apyrase] (13). After incubation under different conditions, cells were processed for immunofluorescence (A) or for protein immunoblotting (B) (14, 16). In both cases, NLS-PK-NES and NLS-PK-NESmut were detected with a monoclonal anti-MYC tag. The nuclear DNA

was visualized by costaining with 4',6'-diamidino-2-phenylindole (DAPI). Photographs corresponding to the different conditions were taken with the same setting parameters. hnRNP C was used as an internal control of a nonexported protein in the same samples. (C) Quantitation of protein immunoblots from four independent experiments was performed with the Bioprint acquisition system and Bioprofil program. Hatched and white columns represent results obtained for NLS-PK-NES and NLS-PK-NESmut, respectively. Values correspond to the ratio between NLS-PK-NES and hnRNP C or NLS-PK-NESmut and hnRNP C contents measured on the same blot and normalized to the ratio measured after incubation in transport buffer without ATP (considered as 100%).

amide gel electrophoresis (PAGE) and protein immunoblotting with an anti-MYC tag and an anti-hnRNP C (Fig. 2, B and C) (15). The hnRNP C protein was used as an internal control of a nonexported protein in both immunofluorescence and protein immunoblotting analyses (10, 16). Neither buffer alone, buffer and ATP, or cytosol treated with apyrase affected the nuclear content of NLS-PK-NES or NLS-PK-NESmut. However, 75% of NLS-PK-NES was exported when both cytosol and ATP were added to permeabilized cells, whereas only 15% of NLS-PK-NESmut was transported under the same condition. In this *in vitro* assay, the replacement of total cytosol by the recombinant proteins required for import (karyopherins, Ran/TC4, and p10) promoted the nuclear import of a karyophilic substrate (BSA-NLS) but did not induce the nuclear export of NLS-PK-NES, which indicates that an essential component for nuclear export was provided by the total extracts (10). Thus, this *in vitro* assay allowed the reconstitution of a NES-, cytosol-, and energy-dependent nuclear export.

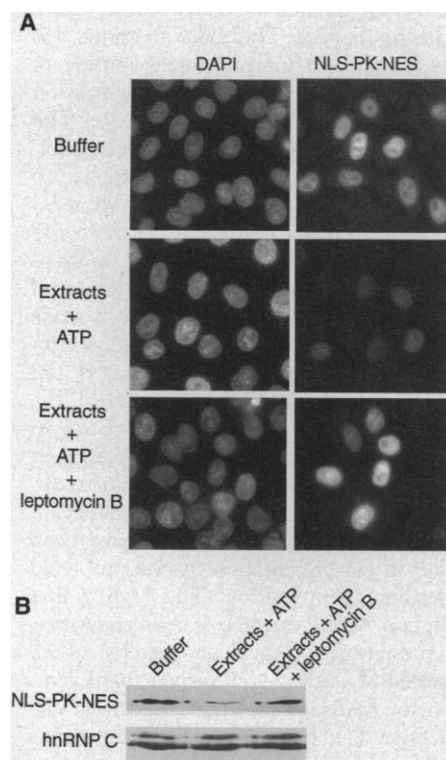


Fig. 3. Leptomycin B inhibits NES-dependent protein nuclear export. *In vitro* nuclear export of NLS-PK-NES was performed as in Fig. 2 in BSA (20 mg/ml) (buffer), in 45% *X. laevis* egg extracts supplemented with ATP (extracts + ATP), or in 45% *X. laevis* egg extracts supplemented with ATP and 200 nM leptomycin B (extracts + ATP + leptomycin B). Nuclear export of NLS-PK-NES was analyzed by indirect immunofluorescence (A) or protein immunoblot (B) with an anti-MYC tag or an anti-hnRNP C.

We next analyzed the role of CRM1-NES interaction in NES-dependent protein export by adding leptomycin B (Fig. 1). Cells producing NLS-PK-NES were permeabilized and treated with cytosol and ATP in the presence or absence of 200 nM leptomycin B (Fig. 3, A and B). Nuclear export of NLS-PK-NES was analyzed by both indirect immunofluorescence and protein immunoblotting. Eighty percent of NLS-PK-NES was exported out of the nucleus with the addition of extracts and ATP, whereas, in the presence of leptomycin B, 90% of the protein stayed in the nucleus. No detectable effect of leptomycin B was observed when the drug was used at a 20 nM concentration (10). Thus, leptomycin B, which inhibits the interaction of CRM1 with NES, was able to block NES-dependent protein export in a similar concentration range. Leptomycin B at a concentration of 2 nM inhibits HIV-1 replication in primary human monocytes or in transient transfection in fibroblasts by preventing Rev function (17), which indicates that CRM1 also interacts with HIV-1 Rev protein. Because the drug could be accumulated by living cells, it may explain why lower concentrations are required for nuclear export inhibition *in vivo* than *in vitro*.

CRM1 thus appears to form a specific complex with NES that is necessary for NES-mediated nuclear protein export. These data suggest that CRM1 could act as an NES receptor involved in nuclear export. Phe-Gly (FG) repeat-containing nucleoporins or related proteins such as RIP have been described as participating in NES-mediated Rev export in both yeast and higher eukaryotic cells. However, direct binding of recombinant Rev to recombinant FG repeats produced in *Escherichia coli* was not detectable *in vitro* (18). The interaction of CRM1 with NES may target the NES-containing substrates to the FG nucleoporins more efficiently. Moreover, CRM1 shares a sequence motif related to the Ran-GTP-binding site of Ran-GTP-binding proteins (4), and both p10 and Ran-GTP, but not Ran-dependent GTP hydrolysis, appear to be required in NES-mediated protein export (19). By analogy with the nuclear import process, Ran or a Ran-binding protein may also regulate the interaction of CRM1-NES-containing protein complexes with the nuclear pore complex before translocation out of the nucleus.

REFERENCES AND NOTES

- D. Görlich, S. Prehn, R. Laskey, E. Hartmann, *Cell* **79**, 767 (1994); J. Moroiaru, G. Blobel, A. Radu, *Proc. Natl. Acad. Sci. U.S.A.* **92**, 2008 (1995); N. Imamoto *et al.*, *EMBO J.* **14**, 3617 (1995); K. Weis, I. W. Mattaj, A. Lamond, *Science* **268**, 1049 (1995); D. Görlich *et al.*, *Curr. Biol.* **5**, 383 (1995); M. Rexach and G. Blobel, *Cell* **83**, 683 (1995); M. K. Iovine, J. L. Watkins, S. R. Wentz, *J. Cell Biol.* **131**, 1699 (1995); J. P. S. Makkerh, C. Dingwall, R. A. Laskey, *Curr. Biol.* **6**, 1025 (1996); V. W. Pollard *et al.*, *Cell* **86**, 985 (1996); J. D. Aitchison, G. Blobel, M. P. Rout, *Science* **274**, 624 (1996); M. Rout, G. Blobel, J. D. Aitchison, *Cell* **89**, 715 (1997).
- M. S. Moore and G. Blobel, *Nature* **365**, 661 (1993); F. Melchior, B. Paschal, J. Evans, L. Gerace, *J. Cell Biol.* **123**, 215 (1993); B. Paschal and L. Gerace, *ibid.* **129**, 925 (1995); U. Nehrbass and G. Blobel, *Science* **272**, 120 (1996).
- Y. Adachi and M. Yanagida, *J. Cell Biol.* **108**, 1195 (1989); T. Toda *et al.*, *Mol. Cell Biol.* **12**, 5474 (1992); M. Fornerod *et al.*, *EMBO J.* **16**, 807 (1997).
- D. Görlich *et al.*, *J. Cell Biol.* **138**, 65 (1997).
- M. Schmidt-Zachmann, C. Dargemont, L. C. Kühn, E. A. Nigg, *Cell* **74**, 493 (1993).
- U. Fischer, J. Huber, W. C. Boelens, I. W. Mattaj, R. Luhrmann, *ibid.* **82**, 475 (1995); W. Wen, J. L. Meinke, R. Y. Tsien, S. S. Taylor, *ibid.*, p. 463; F. Arenzana-Seisdedos *et al.*, *J. Cell Sci.* **110**, 369 (1997); W. M. Michael, M. Choi, G. Dreyfuss, *Cell* **83**, 415 (1995); W. M. Michael, P. S. Eder, G. Dreyfuss, *EMBO J.* **16**, 3587 (1997).
- The complete coding sequence of human CRM1 was amplified by polymerase chain reaction from an HPBALL cell cDNA library and cloned into the Kpn I and Xba I sites of pcDNA3 plasmid (Invitrogen).
- Coupled transcription-translation was performed with the TNT system in a reticulocyte lysate (Promega) supplemented with ³⁵S-methionine and ³⁵S-cysteine (Amersham). Translation products were analyzed by SDS-PAGE and autoradiography. For immunoprecipitation experiments, CRM1 was cotranslated with either wild-type IκBα or IκBα-L234. Five microliters of each TNT reaction was incubated in 40 μl of phosphate-buffered saline (PBS) containing BSA (100 μg/ml) for 30 min at room temperature before being immunoprecipitated with 2.5 μg of either anti-MYC tag or anti-SV5 tag in the presence of 20 μl of protein G-Sepharose (Pharmacia). After being washed in PBS containing 0.1% NP-40, samples were treated with Laemmli sample buffer for 2 min at 95°C and analyzed by 7% SDS-PAGE and fluorography. We obtained NES or mutated NES affinity columns by coupling biotinylated BSA (Pierce) first to sulfosuccinimidyl 4-(N-maleimidomethyl)cyclohexane-1-carboxylate (Pierce) and then to NES peptide (CIQQQLGQLTLENL) or mutated NES peptide (CIQQQAGQATAENA) (9). For each condition, 16 μg of biotinylated BSA coupled to the peptides was bound to 20 μl of streptavidin-agarose. After being washed in PBS, beads were incubated in 40 μl of PBS containing BSA (100 μg/ml), 3 μl of the TNT reaction, and peptides (2 mg/ml) for the competition experiments for 30 min at room temperature. Unbound fractions were collected and sedimented material was extensively washed in PBS before being treated with Laemmli sample buffer for 2 min at 95°C. Samples were analyzed by 7% SDS-PAGE and fluorography.
- Single-letter abbreviations for the amino acid residues are as follows: A, Ala; C, Cys; E, Glu; G, Gly; I, Ile; L, Leu; N, Asn; Q, Gln; and T, Thr.
- B. Ossareh-Nazari, F. Bachelier, C. Dargemont, data not shown.
- M. Yoshida *et al.*, *Exp. Cell Res.* **187**, 150 (1990); K. Nishi *et al.*, *J. Biol. Chem.* **269**, 6320 (1994).
- For transient expression experiments, HeLa cells were trypsinized and resuspended in Dulbecco's modified Eagle's medium supplemented with 10% fetal bovine serum (FBS) and 15 mM Hepes (pH 7.5) at 25 × 10⁶ cells/ml. Fifty microliters of DNA mix (210 mM NaCl, 10 μg of specific DNA, and 30 μg of carrier DNA) was added to 200 μl of cell suspension before electroporation (950 μF, 240 V, with Gene Pulser II; Bio-Rad). Cells were subsequently cultured for 18 hours before analysis. Forty percent of cells were transfected by this protocol.
- S. A. Adam, R. Stern-Marr, L. Gerace, *J. Cell Biol.* **111**, 807 (1990). Transfected cells were permeabilized with digitonin (55 μg/ml; Sigma) in 20 mM Hepes (pH 7.4), 110 mM potassium acetate (pH

7.4), 5 mM NaCl, 2 mM MgCl₂, 1 mM EGTA, 1 mM dithiothreitol (DTT), and protease inhibitors (leupeptin, pepstatin, and aprotinin) for 5 min at 4°C. After being washed twice in the same buffer, cells were incubated for 30 min at 23°C in the different incubation conditions. A high-speed supernatant was prepared from *Xenopus* eggs resuspended in 20 mM Hepes (pH 7.5), 70 mM KCl, 1 mM DTT, and 250 mM sucrose and centrifuged at 13,000g and then at 190,000g. The addition of ATP corresponded to 1 mM ATP, 10 mM creatine phosphate, and creatine phosphokinase (4 U/ml).

14. For indirect immunofluorescence analysis, cells were fixed for 10 min with 2% paraformaldehyde and 0.1% glutaraldehyde and permeabilized with 0.1% Triton X-100 for 5 min. A monoclonal antibody (mAb) to MYC (9E10) was applied for 30 min followed by a 30-min incubation with fluorescein isothiocyanate-conjugated donkey anti-mouse immunoglobulin G (Jackson). Cover slips were

mounted in Moviol (Hoechst, Frankfurt, Germany). Photographs corresponding to the different conditions were taken with the same setting parameters.

15. Cells were treated first with 1 µg of deoxyribonuclease I before being lysed in Laemmli sample buffer containing 8 M urea. Proteins were resolved by 10% SDS-PAGE and transferred to nitrocellulose membrane. Membranes were incubated with mAb 9E10 and an mAb to hnRNP C (4F4), followed by an incubation with anti-mouse coupled to horseradish peroxidase, and finally developed with the chemiluminescence protein immunoblotting reagents (POD, Boehringer Mannheim, Germany). Quantitation of protein immunoblots was performed with the Bio-print acquisition system and Bioprofil program (Vilbert Lourmat).
16. S. Nakielnny and G. Dreyfuss, *J. Cell Biol.* **134**, 1365 (1996).
17. B. Wolff, J. J. Sanglier, Y. Wang, *Chem. Biol.* **4**, 139 (1997).

18. C. C. Fritz, M. L. Zapp, M. R. Green, *Nature* **376**, 530 (1995); F. Stutz, M. Neville, M. Rosbash, *Cell* **82**, 495 (1995); H. P. Bogerd, R. A. Fridell, S. Madore, B. C. Cullen, *ibid.*, p. 485; F. Stutz, E. Izaurralde, I. W. Mattaj, M. Rosbach, *Mol. Cell. Biol.* **16**, 7144 (1996).
19. S. A. Richards, K. L. Carey, I. G. Macara, *Science* **276**, 1842 (1997); T. Tachibana, M. Hieda, T. Sekimoto, Y. Yoneda, *FEBS Lett.* **397**, 177 (1996).
20. We thank Novartis and particularly B. Wolff for leptomycin B; G. Dreyfuss for the anti-hnRNP C; C. Maison for helpful and stimulating discussions; and D. Louvard, J. Salamero, and R. Golsteyn for critical reading of the manuscript. Supported by grants from Action Thematique et Incitative sur Programme et Equipes-CNRS, the Association de Recherche Contre le Cancer, and the European Communities Concerted Action (project: Rocio II).

1 August 1997; accepted 8 September 1997

TECHNICAL COMMENTS

The Possibility of Ice on the Moon

N. J. S. Stacy *et al.* (1) have dealt a blow to the hypothesis that ice deposits may exist in permanently shadowed regions at the lunar poles. Their ground-based radar observations detected several areas with high backscatter cross sections and circular polarization ratios consistent with ice, but in locations that are at least occasionally illuminated by sunlight. These features are associated with walls and rims of small craters; the most likely explanation for their occurrence is high surface roughness at the scale of the radar wavelength. Mercury has regions with similarly anomalous radar properties located near its poles, in permanently shadowed floors of large craters (2). These anomalies have been interpreted as resulting from ices accumulated by cometary and meteoritic bombardment (3). The results of Stacy *et al.* imply an alternative explanation: They may be a result of a difference in texture rather than composition. Such a difference could be caused by their thermal environment.

The sunlit and permanently shadowed regions of Mercury are, respectively, the hottest and coldest surfaces in the solar system that have silicate composition and are subject to meteoroid bombardment. Their responses to impacts should differ accordingly. Hot target material will yield a higher proportion of impact melt, while cold material should have a greater tendency toward brittle fracture, producing fragments that are more angular. Thus, one may expect mature regoliths developed at such different temperatures to have different radar scattering properties, with the colder surface having higher roughness and radar albedo. It is not clear whether this effect would suffice to account for the magnitude

of the radar anomalies observed on Mercury, but this hypothesis could be experimentally tested by hypervelocity impacts into silicate targets at extreme temperatures.

S. J. Weidenschilling
Planetary Science Institute,
620 North 6th Avenue,
Tucson, AZ 85705, USA
E-mail: sjw@psi.edu

REFERENCES

1. N. J. S. Stacy, D. B. Campbell, P. G. Ford, *Science* **276**, 1527 (1997).
2. M. A. Slade, B. J. Butler, D. O. Muhleman, *ibid.* **258**, 635 (1992); J. K. Harmon *et al.*, *Nature* **369**, 213 (1994).
3. A. P. Ingersoll *et al.*, *Icarus* **100**, 40 (1992); R. M. Killen *et al.*, *ibid.* **125**, 195 (1997).

24 June 1997; accepted 28 August 1997

We would like to clarify our understanding of events associated with the 1992 Arecibo observations of the lunar south pole (1) and the Clementine bistatic radar experiment (2). The Clementine team was fully aware of the Arecibo observations before conducting the bistatic radar experiment. Although interpretation of the Arecibo observations was inconclusive, it had been suggested that areas showing high circular polarization ratios (CPRs), observed below the sun line inside the crater containing the south pole, could be underlain by ice (3). Surface roughness was an alternative explanation for the observed high CPR. The Clementine bistatic radar experiment was designed to resolve this ambiguity. Observations over a range of bistatic (phase) angle, β , can distinguish diffuse scattering caused by wavelength-scale roughness from the highly directional coherent backscatter opposition

effect (CBOE), indicative of low-loss targets (for example, ice). This measurement cannot be made from ground-based telescopes. The rationale for bistatic observations is well documented (4).

Clementine observed a CPR peak around $\beta = 0$ near the south pole, consistent with the presence of ice at the surface. This peak was not observed anywhere else on the lunar surface and was isolated to an area within 60 km of the south pole. The radar footprint was fairly broad, and included areas outside of permanent shadow; thus, only a tiny fraction of this area could be underlain by ice. The method used (2) to estimate the area of putative ice deposits is similar to that applied to the polar deposits on Mercury (5). An upper limit on the area of ice deposits of 80 to 135 km² was estimated, assuming contributions to the scattered signal from the total observed area of 45,000 km². If the estimate is made strictly from the surface area that can contribute to the observed CPR peak (that is, the area over which the range of $\beta = \pm 1^\circ$), the area of possible ice deposits is reduced to 7 to 10 km². Given uncertainties in the properties of the putative ice deposits, this estimate can be reconciled with areas showing high CPR in the Arecibo images. We should have been clearer in our presentation in order to avoid misleading interpretation. The high spatial resolution of the Arecibo images show that any possible ice is small and patchy, as we suggested (2). Stacy *et al.* suggest that Clementine and Arecibo measurements are in disagreement (1), but meaningful comparisons can be made only for regions observed at similar incidence and β , normalized to the same area.

A result reported by us (2) for a specific area (80° to 82° south latitude), angle of incidence 84°, $\beta \pm 1$ degree, CPR 0.36 ± 0.01 , is in agreement (3 σ) with the Arecibo near south pole (CPR $0.43 \pm ?$) values, given that no error was stated (1). This correct Clementine near south pole CPR value was not used by Stacy *et al.* (1).